Lysyl Oxidase–Like 2 as a New Poor Prognosis Marker of Squamous Cell Carcinomas

Héctor Peinado,[1] Gema Moreno-Bueno,[1] David Hardisson,[2] Eduardo Pérez-Gómez,[1] Vanesa Santos,[1] Marta Mendiola,[2] Juan Ignacio de Diego,[2] Manuel Nistal,[2] Miguel Quintanilla,[1] Francisco Portillo,[1] and Amparo Cano[1]

[1]Departamento de Bioquímica, Instituto de Investigaciones Biomédicas "Alberto Sols" Consejo Superior de Investigaciones Científicas-Universidad Autónoma de Madrid and [2]Hospital Universitario La Paz, Facultad de Medicina, Universidad Autónoma de Madrid, Madrid, Spain

Abstract

Lysyl oxidase–like 2 (Loxl2) interacts with and stabilizes Snai1 transcription factor, promoting epithelial-mesenchymal transition. Either Loxl2 or Snai1 knock-down blocks tumor growth and induces differentiation, but the specific role of each factor in tumor progression is still unknown. Comparison of the gene expression profiles of the squamous cell carcinoma cell line HaCa4 after knocking-down Loxl2 or Snai1 revealed that a subset of epidermal differentiation genes was specifically up-regulated in Loxl2-silenced cells. In agreement, although both Loxl2- and Snai1-knockdown cells showed reduced *in vivo* invasion, only Loxl2-silenced cells exhibited a skin-like epidermal differentiation program. In addition, we show that expression of Loxl2 and Snai1 correlates with malignant progression in a two-stage mouse skin carcinogenesis model. Furthermore, we found that increased expression of both LOXL2 and SNAI1 correlates with local recurrence in a cohort of 256 human laryngeal squamous cell carcinomas. We describe for the first time that high levels of LOXL2 are associated with decreased overall and disease-free survival in laryngeal squamous cell carcinomas, lung squamous cell carcinoma, and lymph node–negative (N_0) breast adenocarcinomas. Altogether, our results show that LOXL2 can be used as a new poor prognosis indicator in human squamous cell carcinomas promoting malignant transformation by both SNAI1-dependent and SNAI1-independent pathways. [Cancer Res 2008;68(12):4541–50]

Introduction

Metastasis is the most lethal consequence of tumor progression (1). Invasion is the first step during carcinoma metastasis involving changes in cell adhesion, polarity, and remodeling of the extracellular matrix and the cytoskeleton (2). The changes observed during local invasion are associated with a process known as epithelial-mesenchymal transition (EMT), initially described as a critical event during embryogenesis and was recently involved in the metastatic behavior of some carcinomas (3–5). One of the hallmarks of EMT is the loss of E-cadherin expression (6). The mechanisms regulating the transcriptional repression of *E-cadherin* during tumor progression have been thoroughly investigated, especially since the description of Snai1 transcription factor as an E-cadherin repressor (7, 8) and as key regulator of EMT processes during both development and tumor progression (6, 9). We have described that lysyl oxidase–like 2 (LOXL2) interacts with Snai1 and promotes its stabilization by counteracting the action of GSK3β, leading to *E-cadherin* repression and EMT (10, 11). *LOXL2* is a member of the lysyl oxidase (*LOX*) gene family. Five *LOX* family genes have thus far been identified in mammalian genomes encoding the prototypic LOX and LOX-like proteins 1 to 4 (LOXL1, LOXL2, LOXL3, and LOXL4; refs. 12, 13). All the members of the family show a highly conserved catalytic domain located at the COOH terminus, whereas the NH_2 terminus region of the LOX isoforms is more divergent and is thought to determine the individual role and tissue distribution of each isoenzyme (14). The prototypic LOX (EC 1.4.3.13) plays a key role in the biogenesis of the connective tissue catalyzing cross-linkage formation in collagen and elastin components (15). LOX and LOXL1 have been shown to be required for proper elastic fiber homeostasis and cardiovascular system development (16, 17). In addition to its biological role in normal connective tissue function, the LOX family of proteins has recently been implicated in tumorigenesis and metastasis (ref. 18; reviewed in ref. 19). Initial studies showed that LOXL2 overexpression promotes the invasiveness of tumor cells *in vivo* and *in vitro* (20, 21) and its up-regulation has been reported in breast, colon, esophageal, pancreatic, prostatic, and head and neck squamous cell carcinoma (HNSCC) cell lines (4, 10, 20–24). However, few studies on the expression of LOX members in human tumor samples are presently available (19). Particularly, three studies have reported LOXL2 up-regulation in colon and esophageal tumors (25), head-and-neck, and oral squamous cell carcinomas (26, 27), although another study reported the decreased expression of *LOXL2* mRNA in HNSCC (28).

Our previous studies showed that silencing of either Loxl2 or Snai1 blocks tumor growth and induces differentiation (10, 29, 30); however, the specific contribution of each factor to malignant progression and their expression pattern in human tumors are largely unknown. Here, we have investigated the role of LOXL2 and SNAI1 in the regulation of keratinocyte behavior by analyzing the effect of Loxl2 and Snai1 interference in mouse malignant HaCa4 keratinocytes. Our results indicate that Loxl2 promotes malignant progression by both Snai1-dependent and Snai1-independent pathways.

To get further insights in the implication of LOXL2 and SNAI1 in tumor progression, we analyzed their expression in human and mice tumors. The expression of Loxl2 and Snai1 correlated with

Note: Supplementary data for this article are available at Cancer Research Online (http://cancerres.aacrjournals.org/).

H. Peinado and G. Moreno-Bueno contributed equally to this work.

Requests for reprints: Amparo Cano and Francisco Portillo, Instituto de Investigaciones Biomédicas "Alberto Sols" Consejo Superior de Investigaciones Cientificas-Universidad Autónoma de Madrid, Arturo Duperier 4, 28029 Madrid, Spain. Phone: 34-9158-54411/54457; Fax: 34-9158-54401; E-mail: acano@iib.uam.es.

doi:10.1158/0008-5472.CAN-07-6345

malignant progression in the two-stage mouse skin carcinogenesis model. We have examined the expression of both proteins by immunohistochemistry in a cohort of 256 human laryngeal squamous cell carcinomas (LSCC). LSCC comprise the majority (96%) of human laryngeal malignancies (31). Comparative genomic studies have revealed differences in chromosomal pattern and carcinogenic progression between LSCC and other HNSCC (32). However, at present, the biological markers for molecular diagnostics of LSCC have a limited predictive value (reviewed in ref. 33). Among them, it is noteworthy to mention eIF4E overexpression, which predicts recurrence with discrete specificity (34), and loss of p16 expression, which is currently under evaluation (35). Our analysis of SNAI1 and LOXL2 in human LSCC showed that their expression is associated with local recurrence. Moreover, increased staining of LOXL2 with a heterogeneous pattern was also associated with decreased overall and disease-free survival. Our data show for the first time that LOXL2 can be considered as a new marker of poor prognosis in human LSCC. Importantly, the association between high *LOXL2* mRNA expression and poor clinical outcome is also detected by data set analysis in lung squamous cell carcinomas (SCC) and lymph node–negative (N_0) breast adenocarcinoma.

Materials and Methods

Cells and bidimensional cultures. Generation of HaCa4shEGFP, HaCa4shLoxl2, and HaCa4shSnai1 has been previously reported (10, 29). Briefly, HaCa4 cells were transfected with pSuperior vectors containing specific sequences to interfere with mLoxl2 (shLoxl2; ref. 10) or with mSnail (shSnai1; ref. 29), or with short hairpin RNA against enhanced green fluorescent protein (shEGFP), as a control. Stable transfectants were selected with 1 μg/mL of puromycin for 2 to 3 weeks. At least four independent clones were isolated from each transfection (10, 29); one representative clone from each cell line is shown in the figures. Cells were grown in DMEM supplemented with 10% fetal bovine serum, 10 mmol/L of glutamine (Life Technologies), 100 μg/mL of ampicillin, and 32 μg/mL of gentamicin at 37°C in a humidified 5% CO_2 atmosphere.

Patients. The current study was comprised of 256 laryngeal SCCs obtained from surgical patients from the Hospital La Paz, Madrid, Spain. Immunohistochemical studies were carried out on formalin-fixed paraffin-embedded tissue. The series included 249 males and 7 females with a mean age at diagnosis of 60.62 ± 10 years, 33 years old (range, 29–87; Supplementary Table S2). All cases were acquired from the archives of the Department of Pathology, Hospital La Paz with the approval of the head of the Department. All of the tumor samples were diagnosed between 1990 and 1996, and during follow-up for at least 10 years. To validate the external data set mRNA analysis, we analyzed two tumor retrospective samples series from lung SCC (n = 8) and N_0 lymph node breast adenocarcinoma (n = 8), respectively (36, 37). Both series were obtained from the Hospital 12 de Octubre, and the Hospital La Paz, Madrid, Spain. Lung SSC series included three well differentiated, two moderately differentiated, and three poorly differentiated tumors from patients ranging in age from 44 to 67 years. The N_0 breast tumor series included three well differentiated, three moderately differentiated, and two poorly differentiated adenocarcinomas from patients ranging in age from 45 to 50 years old.

Tissue microarray construction. Representative areas from formalin-fixed, paraffin-embedded infiltrating carcinomas were carefully selected on H&E-stained sections and two 1-mm diameter tissue cores were obtained from each specimen. The tissue cores were precisely arrayed into a new paraffin block using a tissue microarray workstation (Beecher Instruments). We constructed eight tissue microarrays containing approximately 32 tumor samples and positive and negative controls.

Mouse skin carcinogenesis. The two-stage mouse skin carcinogenesis (single 7,12-dimethylbenz(a)anthracene application, followed by twice weekly 12-*O*-tetradecanoylphorbol-13-acetate applications for 16 weeks) was performed following standard protocols (38). Tumors were collected at different time periods after initiation and processed for reverse transcription-PCR (RT-PCR) and Western blotting as indicated below.

Microarray gene expression profiles. Microarray experiments were performed using Mouse Whole Genome V2 22 K array G4121B (Agilent Technologies). RNA was isolated using RNeasy Extraction Kit (QIAGen). RNA was labeled and array-hybridized using the Low RNA Linear Amplification Kit and the In Situ Hybridization Kit Plus (Agilent Technologies), respectively. After hybridization and washing, the slides were scanned in an Axon GenePix Scanner (Axon Instruments Inc.) and analyzed using Feature Extraction Software 6.1.1 (Agilent Technologies). Two different RNA samples obtained from each cell line were labeled with Cy5-dUTP. The RNA samples extracted from control cells were marked with Cy3-dUTP (Amersham). Two additional hybridizations were performed using the reciprocal fluorochrome labeling. Two independent clones from each cell line were analyzed, with similar results. The genes whose expression was up-regulated or down-regulated at least 2-fold in HaCa4shLoxl2 or HaCa4shSnai1 with respect to control cells were selected for analysis. A hierarchical clustering method was applied to group the genes and samples on the basis of the similarities in expression, and the unsupervised analyses were visualized using the SOTA and TreeView software assuming Euclidean distances between genes (39).[3] Microarray raw data tables have been deposited in the Gene Expression Omnibus under the accession number GSE8568 (submitter G. Moreno-Bueno).

Class prediction model analysis. For validation of the class prediction model, two independent data set of 51 lung SCC (36) and 286 lymph node negative (N_0) breast adenocarcinoma (37) were analyzed. The microarray and clinical data were obtained from the GEO database,[4] with the accession numbers GSE5123 and GSE2034, respectively. The log-rank test for survival data of each tumor type was obtained to classify samples as high and low expression on the basis of gene expression (LOXL2 and SNAI1) relative to the median across all samples. Statistical analysis of survival was performed with SPSS 14.0.

RT-PCR analysis and Western blotting. Total RNA from cell lines was extracted with Trizol (Invitrogen) and DNaseI treatment. RNA and proteins from tumors were obtained by disruption of the frozen samples with a politron using Tripure reagent (Roche) or radioimmunoprecipitation assay buffer containing protease inhibitor cocktail (Roche). Two micrograms of RNA were employed for cDNA synthesis using oligo-dT and Moloney murine leukemia virus-retrotranscriptase (Promega). Primers for RT-PCR experiments are described in Supplementary Table S3. RT-PCR for *E-cadherin, Snai1, Loxl2*, and *GAPDH* were performed as previously described (10). Proteins from tumors and cell lines were analyzed by Western blot using the enhanced chemiluminescence detection system (GE Heathcare). The antibodies used are listed in Supplementary Table S3.

Organotypic cultures and transplantation assays. Organotypic cultures and transplantation assays on nude mice were performed and processed with two independent clones from each cell line as previously described (40). At least two organotypic cultures of each HaCa4-derived cell clone were studied. Eight mice were used for each HaCa4-derivative cell lines in transplantation experiments. After 1 to 2 weeks of starting the transplantation experiments, four transplants from each group were subjected to immunohistochemical analysis. Mice were housed and maintained under specific pathogen–free conditions and used in accordance with the guidelines approved by the Institutional Animal Care and Use Committee.

Immunofluorescence analysis. The optimal cutting temperature–embedded samples from either the organotypic cultures or *in vivo* transplants were fixed and subjected to immunofluorescence analysis as described (40). The primary antibodies used are described in Supplementary Table S3. The secondary antibodies included goat anti-rat, anti-mouse, or anti-rabbit coupled to Alexa 555 or Alexa 488 (Molecular Probes).

[3] http://bioinfo.cnio.es/cgi-bin/tools/clustering/sotarray
[4] http://www.ncbi.nlm.nih.gov/geo/

Immunohistochemistry of tumors. LOXL2 detection epitope retrieval was performed in a steamer during 3 min in sodium citrate buffer 10 mmol/L (pH 6.0). SNAI1 analysis in tumors was performed as described (41). After endogenous peroxidase blocking, sections were blocked at room temperature for 30 min in PBS 5% normal goat serum, 3% bovine serum albumin, and 1% Triton X-100. Slices were then incubated overnight at 4°C with primary antibodies (diluted in PBS 1% normal goat serum, 1% bovine serum albumin, and 0.1%Triton X-100). Sections were further processed with appropriate secondary antibodies following the LSAB2/horseradish peroxidase Dako cytomation system protocol.

We considered LOXL2 heterogeneous pattern when an intense specific stain (cytoplasm and perinuclear) was observed in at least 20% of the tumor cells, when compared with the faint diffuse staining in the cytoplasm shown in the majority of the cells. In the case of SNAI1, the tumor stain was scored from 0 to 2 (0 negative, <5% of positive cells; 1 low and cytoplasm localization in ~5% to 15% of the cells; 2 cytoplasm-nuclear stain in >15% of the cells). LOXL2 antibody specificity has been probed by immunohistochemistry in xenograft tumors derived from different cell lines (HaCa4 and CarB), which interfered with either an irrelevant sequence (shEGFP) or against Loxl2 (shLoxl2; ref. 10; Supplementary Fig. S1).

Statistical analysis. To test associations between categorical variables, we used the χ^2 or Fisher's exact test. $P < 0.05$ was considered statistically significant. All tests were two-tailed and 95% confidence intervals were adopted. These analyses were carried out using the SPSS 14.0 for statistical program (SPSS, Inc.). We plotted Kaplan-Meir estimates of the surviving (estimated separately for each stratum) and disease-free individuals. We compared survival curves using log-rank test.

Results

Silencing of Loxl2 or Snai1 reduces cell malignancy by different mechanisms. We have previously reported that silencing of Loxl2 or Snai1 has a dramatic effect on the tumorigenic behavior of HaCa4 cells (10, 29). To gain insights into the individual role of Loxl2 and Snai1 in this phenotype, we analyzed HaCa4 mouse SCC cells expressing short hairpin RNA that stably silence the expression of either Loxl2 or Snai1. HaCa4shLoxl2 and HaCa4shSnai1 cells that expressed low levels of Loxl2 or Snai1, respectively (Fig. 1*A*), exhibited increased cell-cell contacts compared with

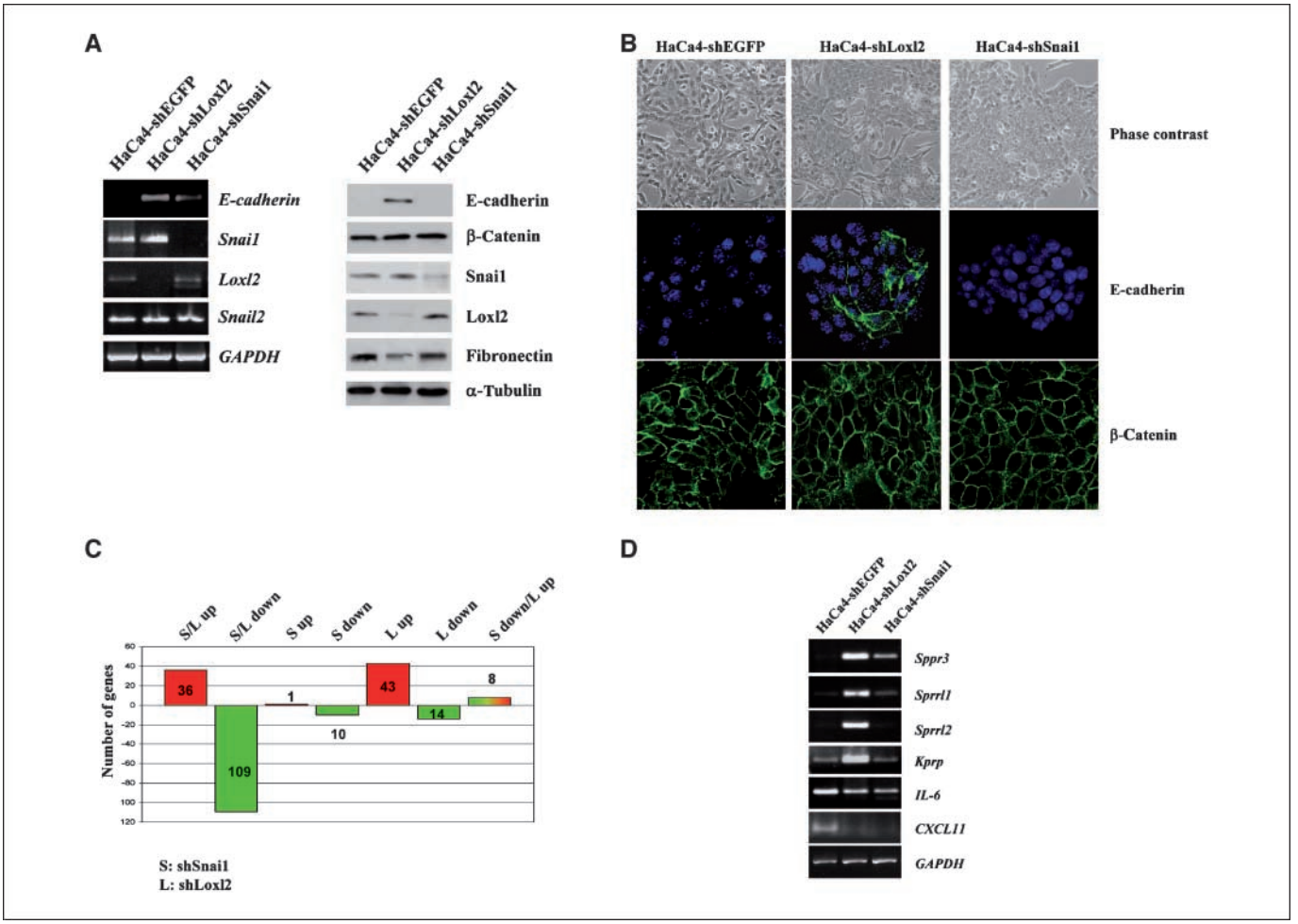

Figure 1. Comparative analysis of the phenotype and gene expression profile of HaCa4 cells after stable silencing of Loxl2 or Snai1. *A,* expression of the indicated genes was analyzed by RT-PCR (*left*) and/or Western blot (*right*) in HaCa4shEGFP or interfered cell lines. *GAPDH* mRNA and α-tubulin levels were analyzed in parallel as a loading control of the amount of cDNAs and protein, respectively. *B,* HaCa4shEGFP, HaCa4shLoxl2, and HaCa4shSnai1 bidimensional culture analyses. Phase contrast images (*top*) and confocal immunofluorescence analysis for E-cadherin (*middle*) or β-catenin (*bottom*). *Bar,* 50 μm. *C,* changes in gene expression profile in HaCa4shSnai1 (*S*) and HaCa4shLoxl2 (*L*) cells compared with the control HaCa4shEGPF cell line; *up,* up-regulated genes (*red columns*); *down,* down-regulated genes (*green columns*); *mixed green and red columns,* differentially expressed genes in analyzed cells. S/L columns indicate the genes up-regulated (*red*) or down-regulated (*green*) in both S and L cell types. *Numbers on the columns,* the number of genes detected in each category. *D,* analysis of mRNA levels of the indicated selected genes in HaCa4shEGFP- and HaCa4-derived cells by RT-PCR. *GAPDH* mRNA levels were analyzed in parallel as a control of the amount of cDNAs.

Table 1. Modified genes involved in cell differentiation (at least 2-fold) in HaCa4-shLoxl2 and HaCa4-shSnai1 compared with HaCa4-shEGFP control cells

Gene symbol	shLoxl2	shSnai1	Description
Epidermal differentiation (n = 21)			
Cnfn	12.3	1.44	Cornifelin
Edg7	−20.75	−10.3	Endothelial differentiation, lysophosphatidic acid G-protein–coupled receptor 7
Figla	−18.75	−13.92	Folliculogenesis specific basic helix-loop-helix
Heyl	−32.4	−12.71	Hairy/enhancer-of-split related with YRPW motif-like
Klk10	23.82	2.25	Kallikrein-related peptidase 10
Klk1b16	−18.69	−2.98	Kallikrein-1–related peptidase b16
Klk7	47.42	1.48	Kallikrein-related peptidase 7 (chymotryptic, stratum corneum)
Klra8	−21.93	−5.74	Killer cell lectin-like receptor, subfamily A, member 8
Kprp	58.82	1.66	Keratinocyte expressed, proline-rich
Krt23	11.16	62.45	Keratin 23
Krt8	2.09	19.08	Keratin 8
Neurod6	−7.17	−7.01	Neurogenic differentiation 6
Ptn	−49.32	−5.55	Pleiotrophin
Sprr2a	16.63	1.63	Small proline-rich protein 2A
Sprr2d	18.84	−1.68	Small proline-rich protein 2D
Sprr2f	19.66	−3.59	Small proline-rich protein 2F
Sprr3	11.63	2.58	Small proline-rich protein 3
Sprrl1	13.93	1.84	Small proline-rich–like 1
Sprrl2	19.68	1.02	Small proline-rich–like 2
Sprrl3	12.5	1.5	Small proline-rich–like 3
Sprrl5	28.84	2.3	Small proline-rich–like 5
EMT-related (n = 15)			
Casq1	−19.45	−1.67	Calsequestrin 1
Epha5	−31.44	−8.71	Eph receptor A5
Fstl1	−11.28	−7.4	Follistatin-like 1
Ifltd1	−16.5	−3.54	Intermediate filament tail domain containing 1
Iyd	−18.32	−5.35	Iodotyrosine deiodinase
Pcdh11x	−12.57	−4.88	Protocadherin 11 X-linked
Pramef12	−16.6	−3.52	PRAME family member 12
S100a8	2.01	−29.51	S100 calcium-binding protein A8 (calgranulin A)
S100a9	6.8	−17.36	S100 calcium-binding protein A9 (calgranulin B)
Serpinb9b	−21.18	−4.01	Serine (or cysteine) peptidase inhibitor, clade B, member 9b
Serpini1	−15.49	−2.56	Serine (or cysteine) peptidase inhibitor, clade I, member 1
Slitrk1	−23.25	−4.61	SLIT and NTRK-like family, member 1
Slitrk6	−14.83	−11.46	SLIT and NTRK-like family, member 6
Tspan1	−15.31	−7.53	Tetraspanin 1
Cdh1	12.77	1.8	Cadherin 1

control cells (HaCa4shEGFP interfered with an irrelevant sequence; Fig. 1*B, top*). HaCa4shLoxl2 cells re-expressed E-cadherin protein (Fig. 1*A, right*) with the typical membrane localization in ~50% of the cell population (Fig. 1*B, middle*); remarkably, these E-cadherin–positive cells seem to differentiate forming multilayers in bidimensional cultures. This pattern was more clearly observed by immunohistochemical staining of the HaCa4-shLoxl2 cultures (Supplementary Fig. S2), which also showed cytoplasmic E-cadherin localization in some cells. Importantly, Loxl2 staining of the same cultures showed almost complete absence of Loxl2 expression in the whole population of HaCa4-shLoxl2, in contrast with the homogeneous cytoplasmic stain of control HaCa4-shEGFP cells (Supplementary Fig. S2). On the other hand, HaCa4shSnai1 cells only express faint levels of *E-cadherin* transcripts (Fig. 1*A, left*), but no protein expression could be detected (Fig. 1*A, right* and *B, middle*), in agreement with our recent observations (10, 29). No significant changes in the expression levels and organization of β-catenin could be observed after Loxl2 or Snai1 silencing in HaCa4 cells (Fig. 1*A, right* and *B, bottom*), indicating the specificity of E-cadherin re-expression in HaCa4shLoxl2 cells. The organization of β-catenin in these cell lines could likely be mediated by P-cadherin, as previously characterized in parental HaCa4 cells (42).

To examine the phenotypic differences of HaCa4shLoxl2 versus HaCa4shSnai1 cells in more detail, gene expression analysis of both cell lines were performed (Fig. 1*C*; Table 1; Supplementary Table S1). A total of 220 genes displayed a >2-fold change in expression in either HaCa4shLoxl2 (L) or HaCa4shSnai1 (S) relative to control HaCa4shEGFP cells. Among them, 145 genes (~66%) were commonly regulated in both cell lines (36 up-regulated and 109 down-regulated; S/L columns, Fig. 1*C*). The remaining genes showed a different expression pattern depending of the cell type. Thus, the expression of 11 genes (5%; 1 up-regulated and 10 down-regulated) was specifically modified in HaCa4shSnai1 cells (S), whereas 57 genes (26%; 43 up-regulated and 14 down-regulated) were exclusively affected in HaCa4shLoxl2 cells (L). These results suggest that, although the majority of the genes (66%) are regulated

by pathways involving both Snai1 and Loxl2, there are a significant number of genes (26%) modified by Loxl2 through Snai1-independent pathways. In addition, eight genes were differentially regulated in both cell lines (mixed color column, Fig. 1*C*). RT-PCR analyses validated the expression of selected genes (Fig. 1*D*). One notable finding was that besides *E-cadherin*, the expression of a great number of cell differentiation genes (16% of the total, 36 genes) is modified by either Loxl2 or Snai1 silencing (Table 1). Moreover, ~60% of them (n = 21) correspond to genes involved in epidermal differentiation. Remarkably, interference of Loxl2 has a much more severe effect than Snai1 silencing on the expression levels of differentiation genes (Table 1), particularly those associated with terminal epidermal differentiation and barrier function such as several members of the small proline-rich protein (Sprr) family (43). These results suggest a potential role for Loxl2 in the regulation of the epidermal differentiation program.

To further characterize the biological consequences of Loxl2 or Snai1 silencing, we analyzed the behavior of HaCa4-interfered cells in organotypic three-dimensional cultures (Fig. 2*A*). Under these growth conditions, control HaCa4shEGFP and HaCa4shSnai1 cells

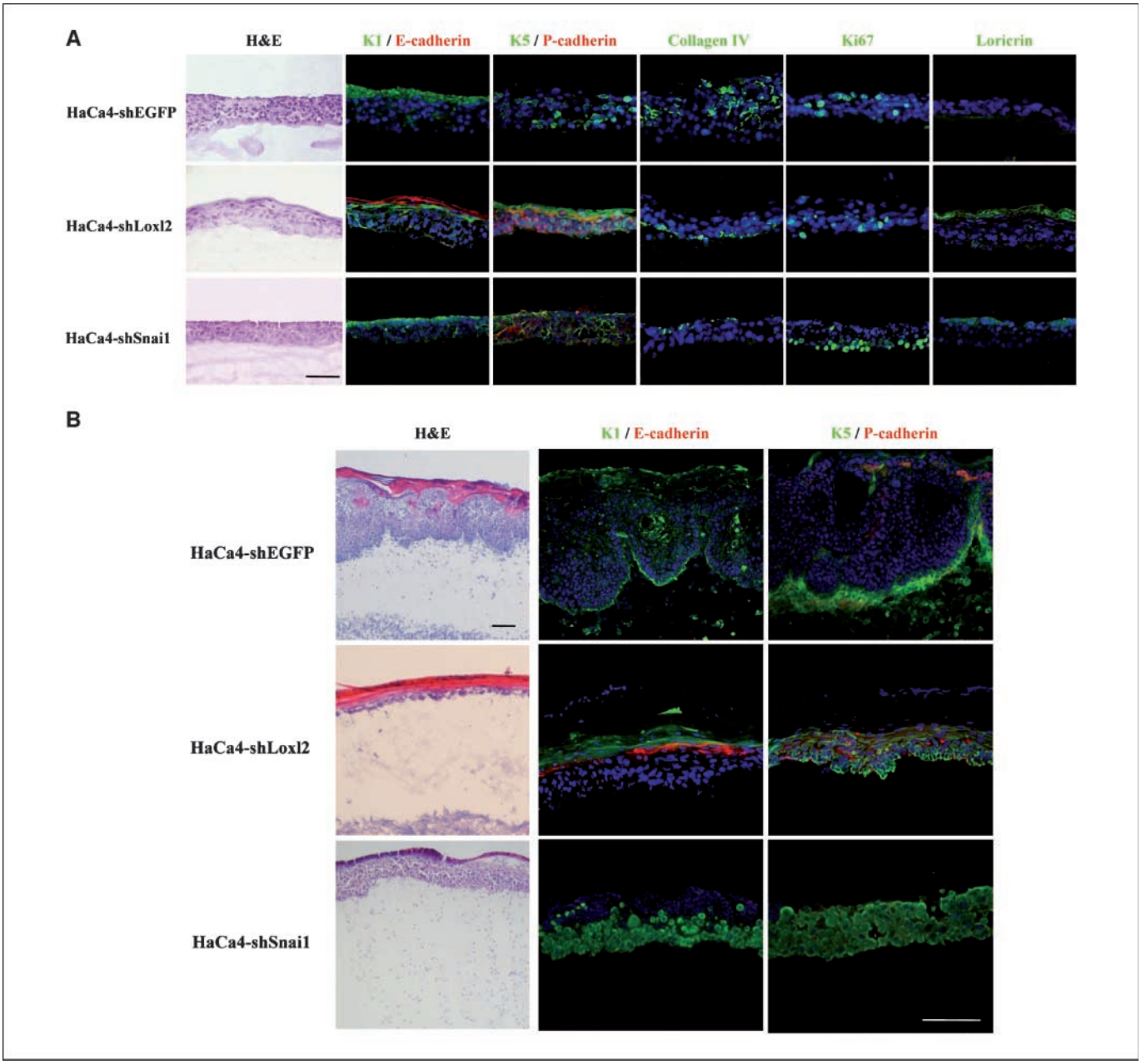

Figure 2. Comparative analysis of the three-dimensional organization and *in vivo* invasion properties of HaCa4 cells after stable silencing of Loxl2 or Snai1. *A,* organotypic three-dimensional cultures of HaCa4shEGFP, HaCa4shLoxl2, and HaCa4shSnai1 after 1 week of culture. Histologic (*H&E*; *left*) and single or double immunofluorescence analysis for the markers indicated above each column (*rest of panels*) were performed; nuclei were stained with 4′,6-diamidino-2-phenylindole (*blue*). *B,* HaCa4shEGFP, HaCa4shLoxl2, and HaCa4shSnai1 were grown on collagen type I gel, transplanted onto the back of nude mice and allowed to grow for 1 week. Sections of each transplantation assay were analyzed by histology (*H&E*; *left*) and double immunofluorescence for the markers indicated above each column; nuclei were stained with 4′,6-diamidino-2-phenylindole (*blue*). One representative example of each type of organotypic culture and transplantation assay is shown. *Bars,* 50 μm. *K1,* cytokeratin 1; *K5,* cytokeratin 5.

behave quite similarly, exhibiting a multilayered epithelioid phenotype with the absence of both E-cadherin and the terminal epidermal differentiation marker loricrin (Fig. 2*A, top* and *bottom*). By contrast, Loxl2 knocked-down cells exhibited an epidermal-like organization with re-expression and organization of E-cadherin at suprabasal layers (Fig. 2*A, middle*). Of note, the expression of the epidermal marker cytokeratin 1 (CK1) was mainly observed in the upper suprabasal layers and loricrin was detected in the upper most keratinized layers in HaCa4shLoxl2 cells (Fig. 2*A, middle*). Noteworthy, in Loxl2-silenced cells, the expression and localization of P-cadherin and collagen IV was detected in the lower basal-like layer (Fig. 2*A, middle*), in contrast with the wider distribution of those markers in most cell layers of HaCa4shSnai1 cultures (Fig. 2*A, bottom*). These findings, together with the low expression levels of the proliferation marker Ki67, which was restricted to the basal layer in HaCa4shLoxl2 cultures (Fig. 2*A, middle*), indicate that Loxl2 silencing is sufficient to induce a skin-like epidermal differentiation phenotype in malignant HaCa4 keratinocytes.

The above hypothesis was further confirmed *in vivo* by analyzing the behavior of HaCa4shLoxl2 and HaCa4shSnai1 in *in vivo* transplantation assays (40, 44, 45). Strong differences in the three-dimensional structural organization and invasiveness induced by both cell types were detected (Fig. 2*B*). HaCa4shEGFP transplants displayed an invasive phenotype with heavy infiltration and a histologic pattern resembling well-differentiated SCC with slight and disorganized expression of E-cadherin and P-cadherin or CK1 (Fig. 2*B, top*). HaCa4shSnai1 cultures exhibited a reduced invasion capacity, but failed to express E-cadherin (Fig. 2*B, lower central panel*). In contrast, HaCa4shLoxl2 transplants showed a fully benign phenotype being unable to invade the collagen gel and adopting a skin-like structure (Fig. 2*B, middle left*). Indeed, HaCa4shLoxl2 transplants express CK1 and E-cadherin in the upper differentiated layers, and CK5 and P-cadherin mainly at the basal cell layer (Fig. 2*B, middle central* and *right panels*). Taken together, these results indicate that both Snai1 and Loxl2 contribute to the invasiveness of SCC cells and, in addition, clearly support a main role for Loxl2 as a negative regulator of the epidermal differentiation program.

Loxl2 and Snai1 are correlated with tumor malignancy. To better understand the potential implication of Loxl2 and Snai1 in tumor progression, we studied the expression of both molecules in tumors derived from the two-stage mouse skin carcinogenesis model, including benign papillomas (Pap) and SCC from well-differentiated (stages I and II) to poorly differentiated (stages III and IV) disease. The expression of Loxl2, Snai1, and the mesenchymal/extracellular marker SPARC (39) was investigated. Results indicated that Loxl2, Snai1, and *SPARC* are expressed in the most advanced tumor stages (Fig. 3), clearly suggesting a correlation between the expression of Loxl2 and Snai1 and tumor malignancy.

To investigate the role of LOXL2 and SNAI1 in human tumors, we studied the expression of both proteins in human LSCC. A series of 256 LSCC with clinical follow-up for at least 10 years (Supplementary Table S2) was analyzed for LOXL2 and SNAI1 expression by immunohistochemistry. The immunohistochemistry of LOXL2 in tumor tissue revealed two different patterns: a diffuse pattern with a faint LOXL2 stain and disperse cytoplasmic distribution (Fig. 4*A, top left*), and a heterogeneous pattern with an increased LOXL2 stain in the cytoplasm or perinuclear envelope of cells distributed in many tumor areas (Fig. 4*A, top right,* see arrows). Moreover, we detected LOXL2 at the tumor front in groups of cells apparently migrating in a collective manner (Fig. 4*A, middle*). In fact, in 86 out 256 tumors (33.6%), the increased heterogeneous expression pattern of LOXL2 was significantly correlated with moderately differentiated and poorly differentiated tumors ($P = 0.016$; Fig. 4*B*). In addition, a highly significant correlation between the heterogeneous pattern of LOXL2 expression and local recurrence of LSCC ($P \leq 0.001$; Fig. 4*B*) was found. The relationship between LOXL2 expression and clinical survival was also investigated using a log-rank test which compares the survival of patients as a function of LOXL2 expression (diffuse versus heterogeneous pattern). A statistically significant difference was found between increased heterogeneous expression of LOXL2 and decreased both overall survival (χ^2, 5.323; 1 *df*, $P = 0.021$; Fig. 5*A, left*) and disease-free survival (χ^2, 6.301; 1 *df*, $P = 0.012$; Fig. 5*A, right*). These results strongly support the hypothesis that LOXL2 can be considered as a new marker of poor prognosis in human LSCC. Additionally, to determine whether the analysis of LOXL2 expression could be applicable to other human tumors as a predictive marker, we examined the correlation between the *LOXL2* mRNA expression level and overall survival in two independent gene expression data sets of 51 lung SCC (36) and

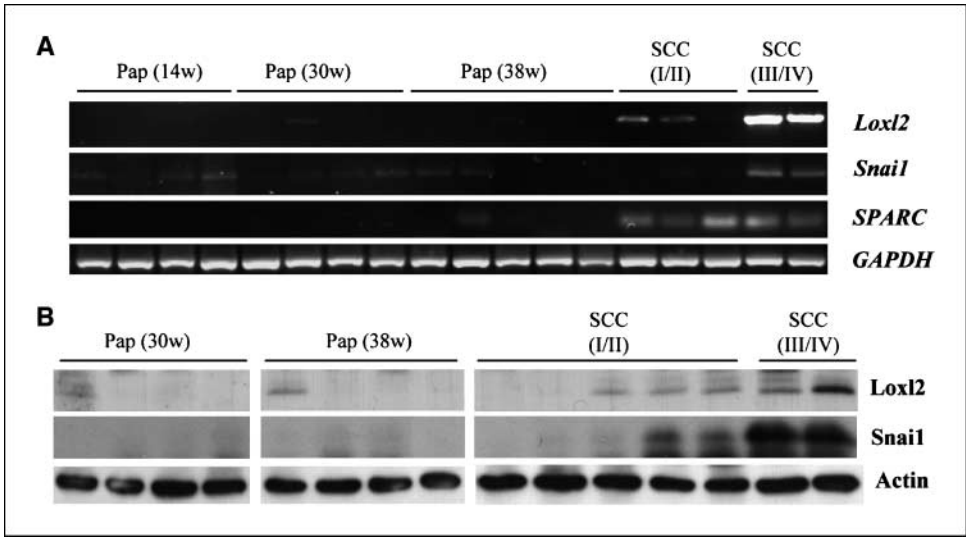

Figure 3. Expression analysis of Loxl2 and Snai1 in tumors derived from mouse skin carcinogenesis. *A,* RT-PCR analyses for the detection of *Loxl2, Snai1*, and *SPARC* mRNA in tumors: papillomas after 14, 30, and 38 weeks (*Pap14w, Pap30w, Pap38w*, respectively) and squamous cell carcinomas (*SCC*), well to moderately differentiated (stages I and II) and poorly differentiated (stages III and IV). Levels of *GAPDH* transcript were used as a control of the amount of cDNAs. *B,* Western blot from the same series of tumors (*Pap30w, Pap38w, SCC I/II*, and *SCC III/IV*) to analyze the protein expression level of Loxl2 and Snai1. Detection of α-actin was used as loading control.

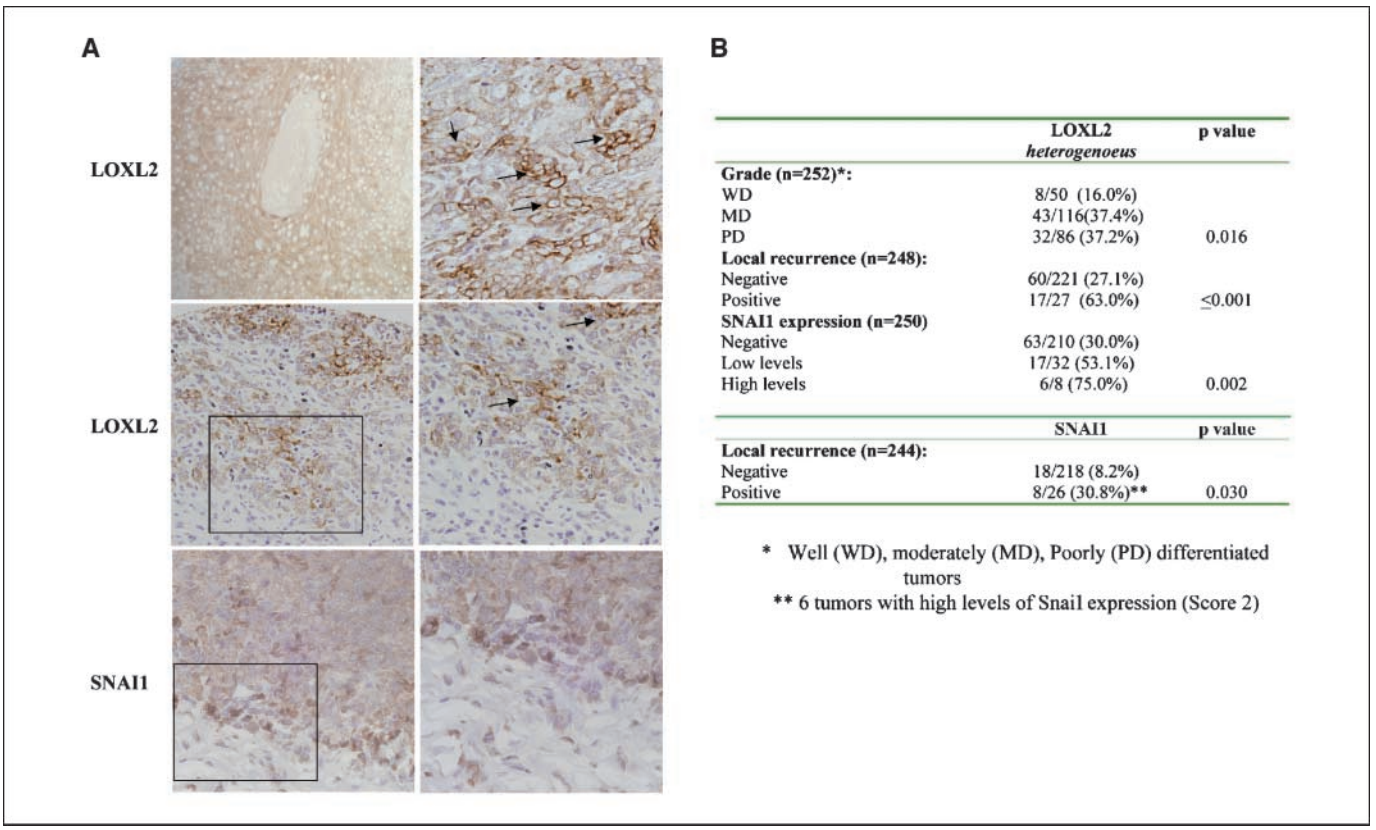

B

	LOXL2 *heterogenoeus*	p value
Grade (n=252)*:		
WD	8/50 (16.0%)	
MD	43/116(37.4%)	
PD	32/86 (37.2%)	0.016
Local recurrence (n=248):		
Negative	60/221 (27.1%)	
Positive	17/27 (63.0%)	≤0.001
SNAI1 expression (n=250)		
Negative	63/210 (30.0%)	
Low levels	17/32 (53.1%)	
High levels	6/8 (75.0%)	0.002

	SNAI1	p value
Local recurrence (n=244):		
Negative	18/218 (8.2%)	
Positive	8/26 (30.8%)**	0.030

* Well (WD), moderately (MD), Poorly (PD) differentiated tumors

** 6 tumors with high levels of Snail expression (Score 2)

Figure 4. Expression analysis of LOXL2 and SNAI1 in LSCC. *A,* immunohistochemical analysis of LOXL2 and SNAI1 expression in representative examples of human LSCC. Diffuse localization of LOXL2 (*top left*). *Arrows,* the heterogeneous pattern of LOXL2 (*top right* and *middle*). High SNAI1 expression is detected in the nuclei and cytoplasm of invading tumor cells (*bottom*). *Middle* and *bottom,* serial sections of the same tumor. *Middle* and *bottom right,* high magnification of the tumor areas indicated by squares in corresponding panels (*left*). *B,* correlations between LOXL2 and SNAI1 expression and clinicopathologic and immunohistochemical features in human LSCC.

286 lymph node–negative (N_0) breast adenocarcinomas (37) using the log-rank test. A statistically significant correlation was found between *LOXL2* expression levels and decreased overall survival in lung SCC (χ^2, 9.05; 1 *df,* P = 0.003; Fig. 5*C*) and lymph node–negative (N_0) breast adenocarcinomas (χ^2, 20.26; 1 *df,* $P \leq 0.001$; Fig. 5*D*).

Analysis of SNAI1 expression in the same cohort of LSCC tumors showed positive staining in ~16% of tumors (40 of 251), but only 8 out 251 tumors (3.1%) exhibited high levels of SNAI1 (Supplementary Table S2), localized both in the nucleus and in the cytoplasm of tumor cells (Fig. 4*A, bottom*). Noteworthy, a significant correlation between SNAI1 expression and increased expression (heterogeneous pattern) of LOXL2 expression was observed (P = 0.002, Fig. 4*B*). In addition, the heterogeneous pattern of LOXL2 was observed in 75% of the tumors showing high levels of SNAI1 (Fig. 4*B*). Interestingly, SNAI1 immunostaining was markedly stronger at the invasion front in apparently actively migrating cells that, in addition, exhibited strong LOXL2 expression (Fig. 4*A, bottom* and *middle*, respectively), as previously reported in cervical SCC and colon carcinomas (41). Importantly, SNAI1 expression was also correlated with the local recurrence of LSCC (P = 0.030; Fig. 4*B*), supporting previous findings in breast carcinoma (46). However, SNAI1 expression was not significantly associated with either overall or disease-free survival in the present series of LSCC (Fig. 5*B*). Analysis of SNAI1 in the data set of lung SCC and lymph node–negative (N_0) breast adenocarcinomas did not find any association between *SNAI1* mRNA expression and clinical survival (data not shown). Nevertheless, we analyzed the expression of LOXL2 and SNAI1 proteins by Western blot in a small subset of tumors representing distinct differentiation grades of lung SCC and lymph node–negative (N_0) breast adenocarcinomas. Results indicated that both SNAI1 and LOXL2 proteins are indeed increased in moderately or poorly differentiated tumors (Supplementary Fig. S3). These preliminary data, together with the analysis of SNAI1 in mouse skin and LSCC tumors, strongly support a model in which SNAI1 is stabilized at the protein level in tumor progression by the action of LOXL2, as we have previously shown *in vitro* (10). Altogether, these observations point to the existence of *in vivo* functional differences between SNAI1 and LOXL2 in relation to tumor progression. Although both molecules cooperate in invasion and local recurrence, LOXL2 plays additional, SNAI1-independent roles in other malignant events that contribute to poor clinical outcome.

Discussion

SNAI1 is an important player of malignancy by mediating key cellular events for tumor progression, like EMT, invasion, and cell survival (5, 6, 9). The mechanisms regulating SNAI1 expression and function have only recently been investigated; in particular, posttranslational modifications affecting SNAI1 protein stability and/or nuclear translocation have attracted much attention (reviewed in ref. 6). Among them, we recently reported that LOXL2, a member of the LOX family, interacts with and stabilizes

Snai1 by a mechanism involving two Snai1 Lys residues and counteracting the action of GSK3β (10, 11). Increased LOXL2 or SNAI1 expression is correlated with the malignant phenotype in cells from mouse squamous and spindle cell carcinomas as well as several human carcinoma cells (7, 10, 29, 47). Moreover, the *in vitro* invasiveness and tumorigenic potential was dramatically blocked in malignant mouse HaCa4 keratinocytes interfered for Loxl2 or Snai1 (10, 29). Nevertheless, those studies do not discriminate between specific or redundant functions of SNAI1 and LOXL2 in tumor progression. To better understand the participation of both molecules, we have performed in-depth *in vitro* and *in vivo* studies of HaCa4 cells with silenced expression of Snai1 or Loxl2. Comparative gene expression analysis of those HaCa4-derived cells showed a cluster of genes that were commonly regulated by Loxl2 and Snai1, but a set of genes was specifically regulated in the Loxl2 knock-down cells. Interestingly, these genes were associated

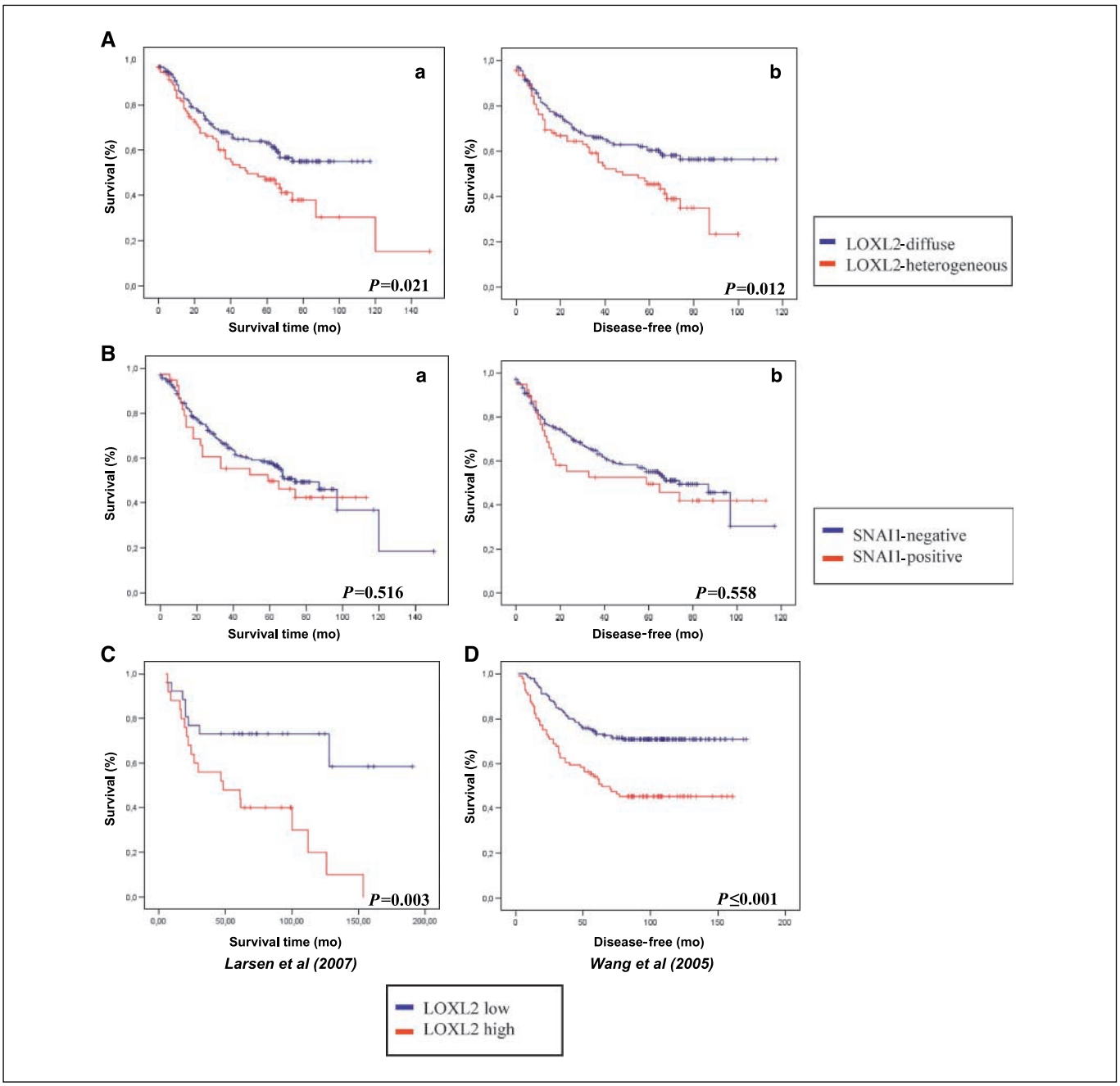

Figure 5. Kaplan-Meier analysis of LOXL2 and SNAI1 expression in LSCC, lung SCC, and lymph node–negative (N_0) breast adenocarcinomas. *A,* Kaplan-Meier plots in the cohort of 256 human LSCC showing that patients with positive (heterogeneous) LOXL2 stain (*red*) had statistically significant decreased overall survival (*left*) and disease-free survival (*right*) compared with patients with negative (diffuse) LOXL2 stain (*blue*). *B,* Kaplan-Meier plots of SNAI1 expression in human LSCC comparing negative (*blue*) and positive (*red*) SNAI1 stain with overall survival (*left*) and disease-free survival (*right*). *C* and *D,* the significant correlation of *LOXL2* expression and overall survival is shown in two independent microarray data sets of 51 lung SCC (ref. 36; *C*) and 286 lymph node–negative (N_0) breast adenocarcinomas (ref. 37; *D*); positive (*red*) and negative (*blue*) expression values of *LOXL2* mRNA were obtained from average of expression ratio. *P* values were derived from log-rank tests.

with terminal epidermal differentiation and barrier function (43, 48), indicating a potential role for Loxl2 in the regulation of epidermal differentiation program. This was further evaluated by analyzing the behavior and homeostasis of the HaCa4-silenced cells in organotypic cultures. As expected, both Loxl2- and Snai1-silenced cells exhibited strongly reduced invasion capacity in organotypic cultures and in *in vivo* transplantation assays. Remarkably, only Loxl2-silenced cells showed expression and organization of both basal/suprabasal epithelial and differentiation markers in a pattern strikingly resembling the mouse skin structure *in vitro* and *in vivo*. These results suggest that Loxl2 influences the Snai1-dependent invasion properties and, perhaps, the Snai1-prosurvival action, but, in addition, Loxl2 has specific functions in the negative control of the epidermal differentiation program, apparently through the direct or indirect regulation of Snai1-independent target genes.

We also studied the expression of Loxl2 and Snai1 in tumor samples derived from mice skin carcinogenesis. This analysis showed a strong correlation between the expression of both proteins and tumor malignancy, and leads us to investigate the expression pattern of LOXL2 and SNAI1 in human tumors. We selected a cohort of LSCC from 256 patients with clinical follow-up for at least 10 years and studied the distribution of LOXL2 and SNAI1 by immunohistochemistry. As mentioned in the Introduction, at present, no reliable molecular markers for the prognosis of that specific type of SCC are available. Our results indicate that LOXL2 expression in LSCC is significantly associated with local recurrence and with decreased clinical and overall survival (see Figs. 4*B* and 5*A*), strongly supporting that LOXL2 can be considered as a new marker of poor prognosis in human LSCC. This remarkable outcome is supported by additional recent observations. First, gene profiling analysis of HNSCC showed that LOXL2 is expressed in a subset of tumors associated with a mesenchymal cell signature (26), and *LOXL2* is considered as one of the 25-gene signatures for oral SCC (27). Second, the analysis of LOXL2 protein levels in colon carcinomas and esophageal tumors showed that LOXL2 protein is increased in the less-differentiated tumors (25). Third, when the *LOXL2* mRNA expression level was used as a variable to predict disease-free survival in a data set of lung SCC (36) and lymph node–negative (N_0) breast adenocarcinomas (37), a significant correlation between *LOXL2* expression and a poor prognosis was detected (see Fig. 5*C* and *D*).

Regarding SNAI1 expression, in the cohort of LSCC tumors, we observed a significant correlation between high levels of SNAI1 expression with local recurrence and the heterogeneous pattern of LOXL2 distribution; however, we did not find any association of SNAI1 expression with other clinicopathologic variables in either the LSCC series (see Fig. 5*B*) or in the data set of lung SCC and lymph node–negative (N_0) breast adenocarcinomas analyzed at the mRNA level. Interestingly, the SNAI1 immunostaining in LSCC was markedly stronger at the invasion front in apparently actively migrating cells, which is in agreement with previously reported results in other types of SCC (41). Moreover, preliminary data analyzing the expression of SNAI1 and LOXL2 proteins in a small subset of lung SCC and lymph node–negative (N_0) breast adenocarcinomas indicated that the expression of both SNAI1 and LOXL2 increases in moderate and poorly differentiated tumors (Supplementary Fig. S3). These new data sheds light on the potential stabilization of SNAI1 by LOXL2 in tumor progression which deserves future analysis.

Altogether, these results confirm that LOXL2, but not SNAI1 expression, predicts poor prognosis in LSCC but in addition they uncover that LOXL2 must function beyond, or apart from, SNAI1 to promote tumor malignancy. This assumption is based on the observation that although the expression of both proteins correlates with local recurrence, only LOXL2 expression associates with poor prognosis. The specific participation of LOXL2 in regulating the reported prosurvival action of Snai1 (49), and thus, potentially local recurrence, is an important aspect that remains to be established. In addition, the elucidation of the Snai1-independent mechanisms through which LOXL2 influences tumor malignancy will be the subject of future studies. In particular, it should be relevant to analyze whether LOXL2 affects the differentiation program of other epithelial tissues, as shown here for epidermis. Whatever the precise molecular mechanisms underlying LOXL2 function, our present data show that LOXL2 can be considered as a new poor prognosis marker in human LSCC. Given the paucity of reliable molecular markers for this highly prevalent laryngeal malignancy, the identification of LOXL2 as a prognostic marker provided here can contribute to improve the clinical treatment of LSCC and point to its potential as a new therapeutic target in LSCC and, perhaps, in other human carcinomas.

Disclosure of Potential Conflicts of Interest

No potential conflicts of interest were disclosed.

Acknowledgments

Received 11/21/2007; revised 3/6/2008; accepted 3/27/2008.

Grant support: Spanish Ministry of Education and Science SAF2004-00361, SAF2007-63051, NAN2004-09230-C04-02, Consolider-Ingenio2010-26102, and the EU MRTN-CT-2004-005428 (A. Cano), the Fundación Mutua Madrileña 2006 and the Spanish Ministry of Education and Science SAF2007-63075 (G. Moreno-Bueno), and the Scientific Foundation of AECC (H. Peinado and M. Mendiola). G. Moreno-Bueno is a junior research investigator of the Ramon y Cajal program 2004.

The costs of publication of this article were defrayed in part by the payment of page charges. This article must therefore be hereby marked *advertisement* in accordance with 18 U.S.C. Section 1734 solely to indicate this fact.

The authors thank A. Montes, M. Julian and M. Hergueta for their valuable contribution, Drs. F. Lopez Rios and J. Palacios for providing the tumor series, and Drs. I. Virtanen and K. Csiszar for providing antibodies.

References

1. Mehlen P, Puisieux A. Metastasis: a question of life or death. Nat Rev Cancer 2006;6:449–58.
2. Gupta GP, Massague J. Cancer metastasis: building a framework. Cell 2006;127:679–95.
3. Kang Y, Massague J. Epithelial-mesenchymal transitions: twist in development and metastasis. Cell 2004; 118:277–9.
4. Thiery JP. Epithelial-mesenchymal transitions in tumour progression. Nat Rev Cancer 2002;2:442–54.
5. Thiery JP, Sleeman JP. Complex networks orchestrate epithelial-mesenchymal transitions. Nat Rev Mol Cell Biol 2006;7:131–42.
6. Peinado H, Olmeda D, Cano A. Snail, Zeb and bHLH factors in tumour progression: an alliance against the epithelial phenotype? Nat Rev Cancer 2007;7:415–28.
7. Cano A, Perez-Moreno MA, Rodrigo I, et al. The transcription factor snail controls epithelial-mesenchymal transitions by repressing E-cadherin expression. Nat Cell Biol 2000;2:76–83.
8. Batlle E, Sancho E, Franci C, et al. The transcription factor snail is a repressor of E-cadherin gene expression in epithelial tumour cells. Nat Cell Biol 2000;2:84–9.
9. Barrallo-Gimeno A, Nieto MA. The Snail genes as inducers of cell movement and survival: implications

in development and cancer. Development 2005;132:3151–61.
10. Peinado H, Iglesias-de la Cruz MC, Olmeda D, et al. A molecular role for lysyl oxidase-like 2 enzyme in snail regulation and tumor progression. EMBO J 2005;24:3446–58.
11. Peinado H, Portillo F, Cano A. Switching on-off Snail: LOXL2 versus GSK3β. Cell Cycle 2005;4:1749–52.
12. Maki JM, Kivirikko KI. Cloning and characterization of a fourth human lysyl oxidase isoenzyme. Biochem J 2001;355:381–7.
13. Csiszar K. Lysyl oxidases: a novel multifunctional amine oxidase family. Prog Nucleic Acid Res Mol Biol 2001;70:1–32.
14. Molnar J, Fong KS, He QP, et al. Structural and functional diversity of lysyl oxidase and the LOX-like proteins. Biochim Biophys Acta 2003;1647:220–4.
15. Lucero HA, Kagan HM. Lysyl oxidase: an oxidative enzyme and effector of cell function. Cell Mol Life Sci 2006;63:2304–16.
16. Maki JM, Rasanen J, Tikkanen H, et al. Inactivation of the lysyl oxidase gene Lox leads to aortic aneurysms, cardiovascular dysfunction, and perinatal death in mice. Circulation 2002;106:2503–9.
17. Liu X, Zhao Y, Gao J, et al. Elastic fiber homeostasis requires lysyl oxidase-like 1 protein. Nat Genet 2004;36:178–82.
18. Erler JT, Bennewith KL, Nicolau M, et al. Lysyl oxidase is essential for hypoxia-induced metastasis. Nature 2006;440:1222–6.
19. Payne SL, Hendrix MJ, Kirschmann DA. Paradoxical roles for lysyl oxidases in cancer—a prospect. J Cell Biochem 2007;101:1338–54.
20. Akiri G, Sabo E, Dafni H, et al. Lysyl oxidase-related protein-1 promotes tumor fibrosis and tumor progression *in vivo*. Cancer Res 2003;63:1657–66.
21. Kirschmann DA, Seftor EA, Fong SF, et al. A molecular role for lysyl oxidase in breast cancer invasion. Cancer Res 2002;62:4478–83.
22. Chung CH, Parker JS, Ely K, et al. Gene expression profiles identify epithelial-to-mesenchymal transition and activation of nuclear factor-κB signaling as characteristics of a high-risk head and neck squamous cell carcinoma. Cancer Res 2006;66:8210–8.
23. Gronborg M, Kristiansen TZ, Iwahori A, et al. Biomarker discovery from pancreatic cancer secretome using a differential proteomic approach. Mol Cell Proteomics 2006;5:157–71.
24. Kiemer AK, Takeuchi K, Quinlan MP. Identification of genes involved in epithelial-mesenchymal transition and tumor progression. Oncogene 2001;20:6679–88.
25. Fong SF, Dietzsch E, Fong KS, et al. Lysyl oxidase-like 2 expression is increased in colon and esophageal tumors and associated with less differentiated colon tumors. Genes Chromosomes Cancer 2007;46:644–55.
26. Chung CH, Parker JS, Karaca G, et al. Molecular classification of head and neck squamous cell carcinomas using patterns of gene expression. Cancer Cell 2004;5:489–500.
27. Ziober AF, Patel KR, Alawi F, et al. Identification of a gene signature for rapid screening of oral squamous cell carcinoma. Clin Cancer Res 2006;12:5960–71.
28. Rost T, Pyritz V, Rathcke IO, Gorogh T, Dunne AA, Werner JA. Reduction of LOX- and LOXL2-mRNA expression in head and neck squamous cell carcinomas. Anticancer Res 2003;23:1565–73.
29. Olmeda D, Jorda M, Peinado H, Fabra A, Cano A. Snail silencing effectively suppresses tumour growth and invasiveness. Oncogene 2007;26:1862–74.
30. Olmeda D, Moreno-Bueno G, Flores JM, Fabra A, Portillo F, Cano A. SNAI1 is required for tumor growth and lymph node metastasis of human breast carcinoma MDA-MB-231 cells. Cancer Res 2007;67:11721–31.
31. Shah JP, Karnell LH, Hoffman HT, et al. Patterns of care for cancer of the larynx in the United States. Arch Otolaryngol Head Neck Surg 1997;123:475–83.
32. Huang Q, Yu GP, McCormick SA, et al. Genetic differences detected by comparative genomic hybridization in head and neck squamous cell carcinomas from different tumor sites: construction of oncogenetic trees for tumor progression. Genes Chromosomes Cancer 2002;34:224–33.
33. Almadori G, Bussu F, Cadoni G, Galli J, Paludetti G, Maurizi M. Molecular markers in laryngeal squamous cell carcinoma: towards an integrated clinicobiological approach. Eur J Cancer 2005;41:683–93.
34. Nathan CO, Sanders K, Abreo FW, Nassar R, Glass J. Correlation of p53 and the proto-oncogene eIF4E in larynx cancers: prognostic implications. Cancer Res 2000;60:3599–604.
35. Sasiadek MM, Stembalska-Kozlowska A, Smigiel R, Ramsey D, Kayademir T, Blin N. Impairment of MLH1 and CDKN2A in oncogenesis of laryngeal cancer. Br J Cancer 2004;90:1594–9.
36. Larsen JE, Pavey SJ, Passmore LH, et al. Expression profiling defines a recurrence signature in lung squamous cell carcinoma. Carcinogenesis 2007;28:760–6.
37. Wang Y, Klijn JG, Zhang Y, et al. Gene-expression profiles to predict distant metastasis of lymph-node-negative primary breast cancer. Lancet 2005;365:671–9.
38. Quintanilla M, Brown K, Ramsden M, Balmain A. Carcinogen-specific mutation and amplification of Ha-ras during mouse skin carcinogenesis. Nature 1986;322:78–80.
39. Moreno-Bueno G, Cubillo E, Sarrio D, et al. Genetic profiling of epithelial cells expressing E-cadherin repressors reveals a distinct role for snail, slug, and E-47 factors in epithelial-mesenchymal transition. Cancer Res 2006;66:9543–56.
40. Peinado H, Marin F, Cubillo E, et al. Snail and E47 repressors of E-cadherin induce distinct invasive and angiogenic properties *in vivo*. J Cell Sci 2004;117:2827–39.
41. Franci C, Takkunen M, Dave N, et al. Expression of Snail protein in tumor-stroma interface. Oncogene 2006;25:5134–44.
42. Navarro P, Gomez M, Pizarro A, Gamallo C, Quintanilla M, Cano A. A role for the E-cadherin cell-cell adhesion molecule during tumor progression of mouse epidermal carcinogenesis. J Cell Biol 1991;115:517–33.
43. Hohl D, de Viragh PA, Amiguet-Barras F, Gibbs S, Backendorf C, Huber M. The small proline-rich proteins constitute a multigene family of differentially regulated cornified cell envelope precursor proteins. J Invest Dermatol 1995;104:902–9.
44. Boukamp P, Stanbridge EJ, Foo DY, Cerutti PA, Fusenig NE. c-Ha-ras oncogene expression in immortalized human keratinocytes (HaCaT) alters growth potential *in vivo* but lacks correlation with malignancy. Cancer Res 1990;50:2840–7.
45. Skobe M, Rockwell P, Goldstein N, Vosseler S, Fusenig NE. Halting angiogenesis suppresses carcinoma cell invasion. Nat Med 1997;3:1222–7.
46. Moody SE, Perez D, Pan TC, et al. The transcriptional repressor Snail promotes mammary tumor recurrence. Cancer Cell 2005;8:197–209.
47. Fraga MF, Herranz M, Espada J, et al. A mouse skin multistage carcinogenesis model reflects the aberrant DNA methylation patterns of human tumors. Cancer Res 2004;64:5527–34.
48. Patel S, Kartasova T, Segre JA. Mouse Sprr locus: a tandem array of coordinately regulated genes. Mamm Genome 2003;14:140–8.
49. Vega S, Morales AV, Ocana OH, Valdes F, Fabregat I, Nieto MA. Snail blocks the cell cycle and confers resistance to cell death. Genes Dev 2004;18:1131–43.

Lysyl Oxidase–Like 2 as a New Poor Prognosis Marker of Squamous Cell Carcinomas

Héctor Peinado, Gema Moreno-Bueno, David Hardisson, et al.

Cancer Res 2008;68:4541-4550.